Hindawi
Journal of Electrical and Computer Engineering
Volume 2018, Article ID 2156980, 10 pages
https://doi.org/10.1155/2018/2156980

Research Article

EPS Current Tracking Method Research Based on Hybrid Sensitivity H_∞ Control Algorithm

Hairong Wu,[1] Guangfei Xu,[1,2] Jian Wu ,[1] Xue Han,[3] Jiwei Feng,[1] Shifu Liu,[1] and Linglong Bu[2]

[1]*School of Mechanical and Automotive Engineering, Liaocheng University, Liaocheng City, Shandong Province 252000, China*
[2]*Modern Agricultural Demonstration Garden, Liaocheng Academy of Agricultural Sciences, Liaocheng City, Shandong Province 252000, China*
[3]*Economic & Technology Research Institute, State Grid Shandong Electric Power Company, Jinan City, Shandong Province 250000, China*

Correspondence should be addressed to Jian Wu; wujian1982@mail.tsinghua.edu.cn

Received 20 September 2017; Accepted 13 February 2018; Published 4 June 2018

Academic Editor: Ephraim Suhir

For electric power steering system (EPS), road interference, noise of the sensor, and the uncertainty of the steering system may make EPS control effect and the driver's road sense worse. EPS system which takes advantage of good current tracking ability, good anti-interference ability, and good operation stability is becoming more and more important in automotive research. The traditional H_∞ control algorithm can solve the system uncertainty theoretically, but it cannot solve the contradiction between robustness and performance without considering the performance of the system. Therefore, this paper proposes a EPS current tracking method based on the hybrid sensitivity H_∞ control algorithm, which takes the current tracking performance as one of the control objectives, so that the system can maximize the robustness and performance. Firstly, the dynamic model of EPS is established. Then, the two-degree-of-freedom vehicle model and tire model are introduced. The state space equation of the system is constructed on the basis of the system state space with random disturbance signals, the hybrid sensitivity H_∞ controller is designed in the sensitivity index design, and the proposed algorithm can use weighting function to minimize the performance of the current tracking error as well as the robustness of the yaw rate error in response to robustness. Simulation analysis and experimental verification of EPS system are also carried out. The results show that the control method of the hybrid sensitivity H_∞ can better achieve EPS target current tracking, effectively suppress the effect of external interference and noise, improve the system performance and robustness, ensure the driver get good road sense, and improve the system of steering stability.

1. Introduction

Electric power steering (EPS) system is the core technology of the automobile steering system. It is the key component of intelligent driving. It has the advantages of portability, agility, energy saving, environmental protection, and convenient installation. The EPS system is based on the mechanical steering system, and the auxiliary motor is added to control the motor to provide the auxiliary torque to achieve the purpose of power steering. Great progress has been made in EPS system and it has been widely used in automobile industry. The EPS control based on the classical control theory can realize the power steering function, but the EPS feel is not as well as hydraulic power system (HPS) [1]. It cannot restrain the disturbance caused by nonlinear factors due to the uncertainties of the steering system.

Classical control theory, modern control theory, and advanced control theory have been applied to the study of EPS system one after another. Classical control theory was first applied to EPS. Tan Guangxing et al. [2] proposed a kind of EPS control based on immune fuzzy PID. This kind of control based on fuzzy PID can greatly improve EPS power steering performance and portability. Then, PID control of EPS is further developed by using modern control theory. Zhang jianwei et al. [3] proposed a PID control strategy based on genetic algorithm, which is used to optimize the PID controller parameters by using genetic algorithm so as to achieve better control effect.

The above research does not fundamentally solve the current tracking problem, especially anti-interference and robustness problem. Then, the robustness of EPS system has become the focus of research. In order to improve the anti-interference ability of EPS system, advanced control theory is applied to EPS research. Various anti-interference algorithms have been studied experimentally. Qiu Ming et al. [4] studied the EPS based on the control principle and discussed the uncertainty of the system model and the method of minimizing interference to achieve robust control of the EPS. Wang Qirui et al. [5] studied the standard control problem of EPS and designed the robust controller for the road sense. Zhao Wanzhong et al. [6] studied EPS based on H_2/H_∞ hybrid control using H_∞ to minimize the impact of interference on the output and simultaneously carry out the H_2 optimization. Weng Jingliang et al. [7] studied the robust control strategy of EPS based on handling stability. The stability and tracking problem of the system were transformed into a hybrid sensitivity problem. She Guoqin et al. [8] studied the robust control of EPS and its influence on handling stability by using hybrid sensitivity method. Chen long et al. [9] designed a new μ controller by selecting the related performance indexes based on μ synthesis theory and robust control method. The stability and safety of vehicle are improved effectively. Frédéric Wilhelm et al. [10] considered the effects of friction in EPS and proposed an active compensation control strategy which could estimate the internal friction of the system and compensate for it through the motor input. It is composed of two feedback loops: internal loop for system friction estimation and external loop for minimizing the tracking error. Ying-Chih Hung et al. [11] proposed a wavelet fuzzy neural network using asymmetric membership function (WFNN-AMF) with improved differential evolution (IDE) algorithm to control the EPS. It improved the stability and comfort of the vehicle to great extent. But the performance of EPS is given less attention. Wonhee Kim et al. [12] proposed a lane-keeping system of automated vehicle based on EPS which takes unknown parameters and external disturbance, along with their derivatives into the designment of the augmented observer and nonlinear damping controller. Alaa et al. [13] studied a kind of new EPS control strategy. They, respectively, test the reference target and determine the reference model and finally realize the EPS control by using the two-level synovial control strategy to track the motor corner. Dongwook Lee et al. [14] and Cassio T. Faria et al. [15] all identified the external disturbance, nonlinearity, and uncertainty of EPS system, and the controller design is carried out based on them. Some results have been achieved.

The studies mentioned above about the EPS control achieved considerable effect, but there should be more in-depth study on current tracking performance which is the main indicators of the controller. These studies are based on the simulation level, so they can not verify the real effect of the algorithm due to the inevitable gap between the designed algorithm model and the actual steering system. Therefore, a H_∞ controller based on hybrid sensitivity is designed and the controller is used in the actual steering system.

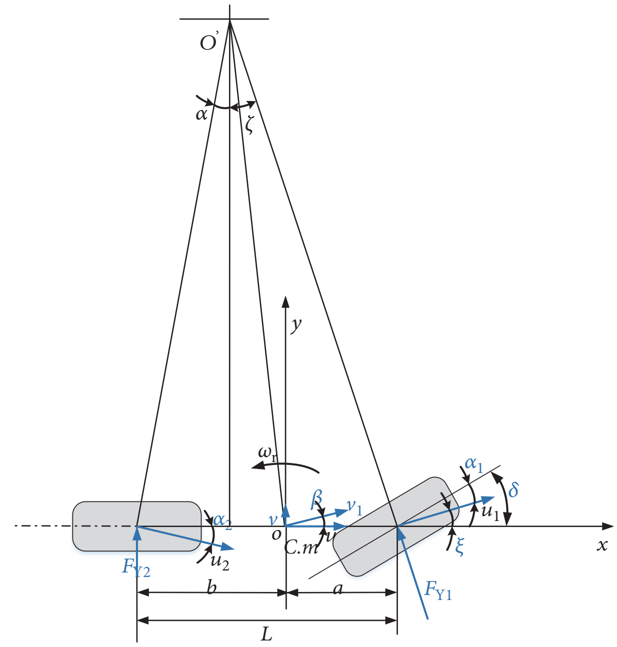

Figure 1: Two-degree-of-freedom vehicle model.

This paper is arranged as follows. The second section presents the two-degree-of-freedom vehicle model, EPS steering system model, and others. The third section describes the design of the new hybrid sensitivity H_∞ controller. In the fourth section, the simulation results of the PID and the new hybrid sensitivity H_∞ control strategy are shown. Then, the fifth section is the comparison of experimental results between two control strategies applied on the real experimental bench. Finally, the conclusions are shown in the sixth section.

2. Mathematical Model of EPS System

2.1. Two-Degree-of-Freedom Vehicle Model. In this paper, the steering performance of automobile is studied, so a simplified model of vehicle with 2 degrees of freedom is presented [16] in Figure 1.

The model's motion differential equation is

$$(k_1 + k_2)\beta + \frac{1}{u}(ak_1 - bk_2)\omega_r - k_1\delta = m(\dot{\beta} + \omega_r) \quad (1)$$

$$(ak_1 - bk_2)\beta + \frac{1}{u}(a^2k_1 + b^2k_2)\omega_r - ak_1\delta = I_z\dot{\omega}_r \quad (2)$$

k_1 and k_2 are, respectively, the stiffness of front and rear wheels. β means sideslip angle of vehicle center of mass. u is vehicle centroid velocity. a and b are, respectively, the distance between the car and the center of mass. ω_r means yaw speed for car. δ means front wheel corner. m means mass of vehicle. I_z is the moment of inertia of the car around the z-axis.

2.2. EPS Steering System Model. For the convenience of study, this paper simplifies the front wheel and steering gear to steering shaft [17]. We focus on the situation that the relevent forces are equivalent to the steering axis. On the basis of the reliability of the model, the relation between the input and output variables is established [18]. EPS simplified model is shown in Figure 2.

In Figure 2, T_h means torque input for steering wheel. T_s means measuring torque of torque sensor. T_m means electromagnetic torque of motor. T_r is the steering resistance moment of the road equivalent to the torque on the pinion (gear ratio is N). $N_1 T_m$ is the motor torque acting on the steering shaft torque. N_1 is the drive ratio which is the steering shaft to the motor. θ_h is steering angle. θ_m is the angle of motor. δ_1 is steering shaft angle. J_h is the moment of inertia of steering wheel. J_p is the moment of inertia converted to steering shaft. B_p is the equivalent damping coefficient of system friction.

2.2.1. The Steering Shaft Model. The dynamic analysis of the wheel part above the torque sensor can be

$$(k_1 + k_2)\beta + \frac{1}{u}(ak_1 - bk_2)\omega_r - k_1\delta = m(\dot{\beta} + \omega_r) \tag{3}$$

Dynamic analysis of the steering shaft below the torque sensor is available by

$$K_s(\theta_h - \delta_1) + N_1 T_m - T_r = J_p\ddot{\delta}_1 + B_p\delta_1 \tag{4}$$

K_s is torsion bar stiffness of sensor.

2.2.2. Electrical Machinery Model. The system uses a brushed DC motor. The differential equation can be obtained by Holzer's law of voltage:

$$u_a = L_a\dot{I}_a + R_a I_a + K_b\dot{\theta}_m \tag{5}$$

$$\dot{\theta}_m = N_1\dot{\delta}_1 \tag{6}$$

$$T_m = K_a I_a \tag{7}$$

u_a is the motor terminal voltage. R_a is armature resistance. K_a is torque coefficient of motor. K_b is coefficient of back electromotive force of motor. L_a is inductance coefficient of motor. I_a is motor current.

2.2.3. Steering Resistance Moment Calculation. At the small angle, the tire deformation is approximately linear. The steering resistance moment of the pinion acting on the road through the tire [19] is

$$T_r = \frac{2}{N}dk_1\left(\frac{\delta_1}{N} - a\frac{\omega_r}{u} - \beta\right) \tag{8}$$

d is pneumatic trail.

2.2.4. The State Equation of the System. The state equation of the system can be obtained by formulas (1) ~ (8):

$$\dot{X} = AX + B_1\omega + B_2U \tag{9}$$

Take state variables as $X = \left[\dot{\theta}_h \;\; \theta_h \;\; I_a \;\; \dot{\delta}_1 \;\; \delta_1 \;\; \beta \;\; \omega_r\right]^T$. The control input is $U = [T_h \;\; u_a]^T$. The road signal input is $\omega = s_0\delta(t)$. s_0 is coefficient of interference intensity. $\delta(t)$ is pavement interference noise.

Among them, the coefficient matrices A, B are

$$A = \begin{bmatrix} -\frac{B_h}{J_h} & -\frac{K_s}{J_h} & 0 & 0 & \frac{K_s}{J_h} & 0 & 0 \\ 1 & 0 & 0 & 0 & 0 & 0 & 0 \\ 0 & 0 & -\frac{R_a}{L_a} & -\frac{N_1K_b}{L_a} & 0 & 0 & 0 \\ 0 & \frac{K_s}{J_p} & \frac{N_1K_a}{J_p} & -\frac{B_p}{J_p} & -\frac{K_s}{J_p} - \frac{2dK_1}{N^2J_p} & \frac{2adK_1}{NuJ_p} & \frac{2dK_1}{NJ_p} \\ 0 & 0 & 0 & 1 & 0 & 0 & 0 \\ 0 & 0 & 0 & 0 & -\frac{k_1}{Nm} & \frac{k_1+k_2}{m} & \frac{ak_1-bk_2}{mu} - 1 \\ 0 & 0 & 0 & 0 & -\frac{ak_1}{NI_Z} & \frac{ak_1-bk_2}{I_Z} & \frac{a^2k_1+b^2k_2}{uI_Z} \end{bmatrix} \tag{10}$$

$$B_1 = \begin{bmatrix}0 & 0 & 0 & 1 & 0 & 0 & 0\end{bmatrix}^T$$

$$B_2 = \begin{bmatrix} \frac{1}{J_h} & 0 & 0 & 0 & 0 & 0 & 0 \\ 0 & 0 & 1 & 0 & 0 & 0 & 0 \end{bmatrix}^T$$

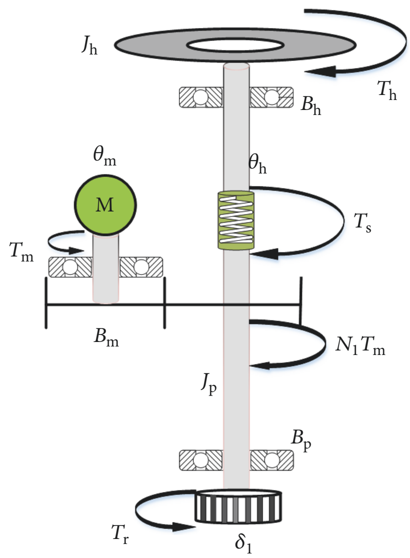

FIGURE 2: Schematic diagram of a simplified dynamic EPS system.

Take the output variable of the system as $Y = [I_a\ T_s\ \omega_r\ \delta_1\ T_r]$.

The output equation of the system is

$$Y = CX + DU \tag{11}$$

where

$$C = \begin{bmatrix} 0 & 0 & 1 & 0 & 0 & 0 & 0 \\ 0 & K_s & 0 & 0 & -K_s & 0 & 0 \\ 0 & 0 & 0 & 0 & 0 & 0 & 1 \\ 0 & 0 & 0 & 0 & 1 & 0 & 0 \\ 0 & 0 & 0 & 0 & \dfrac{2dk_1}{N^2} & -\dfrac{2adk_1}{Nu} & \dfrac{2dk_1}{N} \end{bmatrix} \tag{12}$$

$$D = [0\ \ 0\ \ 0\ \ 0\ \ 0]^T$$

3. Design of H_∞ Controller Based on EPS

3.1. Hybrid Sensitivity Design Problem. The hybrid sensitivity design structure of EPS system is shown in Figure 3. $P(s)$ is the nominal space model of the system: the state space model of EPS system model. u_1 is the reference input system, including target current, ideal torque, sensor measurement, and ideal yaw rate. u_2 is system control input: the input voltage of the motor. $e(t)$ is the error of the signal, including the deviation of the target current from the actual current, the sensor measurement deviation, and yaw rate deviation. $u(t)$ is the control input, and y is the system output, including the actual current, the sensor torque, and the yaw rate. z is the system output evaluation, mainly referring to the impact of interference on control error (the current tracking performance of sensor, interference suppression, and handling stability), energy control input, and robust stability. W_S is sensitivity weighting factor. W_R is input sensitivity weighting factor, W_T is sensitivity weighted factor, and $K(s)$ is the controller of the system [20].

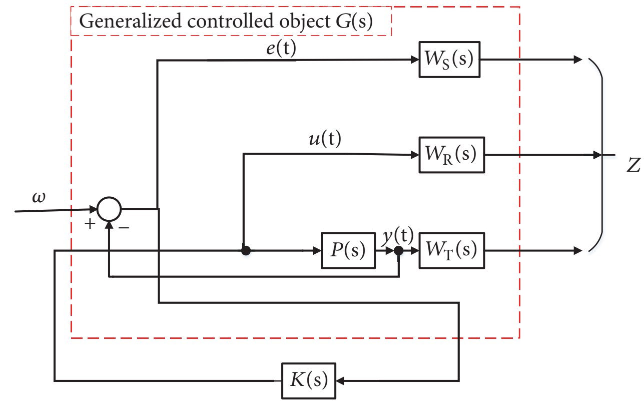

FIGURE 3: Block diagram of hybrid sensitivity design of EPS system.

The sensitivity control function S, the input sensitivity function R, and the complement sensitivity function T are included in the design of the hybrid sensitivity H_∞ control system [21]. Its Laplasse transform [22], respectively, is

$$S(s) = [I + P(s)K(s)]^{-1} \tag{13}$$

$$R(s) = [I + P(s)K(s)]^{-1} K(s) \tag{14}$$

$$T(s) = [I + P(s)K(s)]^{-1} K(s) P(s) \tag{15}$$

I is the unit matrix.

$\|S\|_\infty$ is the infinite norm of the sensitivity function S and it represents the tracking performance of the closed-loop control system to the target. In order to improve the tracking performance of the system, $\|S\|_\infty$ should be as small as possible. $\|T\|_\infty$ is the infinite norm of the complement sensitivity function T and it represents the measure of the perturbation allowed by the closed-loop system. In order to ensure the robustness of the system, $\|T\|_\infty$ should be as small as possible. However, there is a limitation of $S + T = I$ at the same system frequency, so $\|S\|_\infty$ and $\|T\|_\infty$ cannot reach the minimum at the same time [21]. By introducing the sensitivity weighting matrix, W_S, and the complement sensitivity weighting matrix, W_T, the relative performance and stability of the system can be achieved. In addition, in order to avoid the actuator (motor) saturation or overload, the input sensitivity function weighting matrix, W_R, is introduced to limit the overoutput [23].

The hybrid sensitivity design problem is transformed into a controller $K(s)$ about system stability, disturbance rejection, and current tracking problems. The closed-loop control system from ω to z, including the generalized controlled object $G(s)$, is stable and minimal. It can be described as

$$\|T_{z\omega}\|_\infty = \left\| \begin{matrix} W_S S \\ W_R R \\ W_T T \end{matrix} \right\|_\infty \le 1 \tag{16}$$

The hybrid sensitivity control problem can be reduced to a H_∞ control problem. For generalized space G,

$$G = \begin{bmatrix} G_{11} & G_{12} \\ G_{21} & G_{22} \end{bmatrix} = \begin{bmatrix} W_S & -W_S P \\ 0 & W_R \\ 0 & W_T P \\ 0 & P \end{bmatrix} \quad (17)$$

The solution of the control problem is to find controller K, stabilize G, and make $\|F_l(G,K)\|_\infty < \gamma$.

3.2. The Design of Evaluation Index

3.2.1. Tracking Performance. Due to the influence of sensor noise and other system uncertainties, there is a certain deviation between the actual auxiliary current I_a and the target current value $I_a{}^*$. It can be shown as

$$e_1 = I_a^* - I_a \quad (18)$$

In order to reduce the effect of error and improve the current tracking performance, this paper makes a weighted control of the current deviation between the actual current and the target current obtained through the help characteristic curve to obtain better tracking performance.

It can be expressed as

$$\|W_{s1} e_1\|_\infty = \|W_{s1} (I_a^* - I_a)\|_\infty \quad (19)$$

W_{s1} is the current tracking weighting function.

3.2.2. Road Feeling. Road feeling is the reaction of pavement information on the steering wheel. The pavement is measured by the reaction of torque sensor by fixing the steering wheel. We use T_s to represent the measurement of torque sensor. The road surface information is reflected by the steering resistance moment T_r. To get good road sense, we need to control the error between the two.

It can be expressed as

$$\|W_{s2} e_2\|_\infty = \|W_{s2} (T_s - \varphi T_r)\|_\infty \quad (20)$$

φ is the road sense coefficient and W_{s2} is the road sense weighting function [24].

3.2.3. Handling Stability. The handling stability is mainly reflected in the changes of yaw rate. The target value of yaw rate is determined by the steady-state yaw rate gain function [20].

$$\omega_r^* = \frac{u/L}{1 + Ku^2} \delta_1 \quad (21)$$

where

$$K = \frac{m}{L^2} \left(\frac{a}{k_2} - \frac{b}{k_1} \right) \quad (22)$$

In order to obtain better handling and stability, the deviation between the actual yaw rate ω_r and the target yaw rate ω_r is controlled as

$$\|W_{S3} e_3\|_\infty = \|W_{S3} (\omega_r^* - \omega_r)\|_\infty \quad (23)$$

W_{S3} is the stability weighting function.

3.2.4. Avoiding Current Overload. In order to avoid the excessive input current of the motor, the function of input W_R is introduced. It makes $\|W_R u_a\|_\infty$ as small as possible to reduce energy consumption and device loss.

3.2.5. The Robust Stability of the System. In order to avoid the system instability due to the performance of the system, the output of the system is weighted by $\|W_T Y\|_\infty$.

W_T is the complementary sensitivity weighting factor.

3.3. Selection of Weighting Function. The selection of weighting function reflects the requirement of the performance index of the control system and the choice should be based on the specific control target and the control requirement.

In general, the order of a weighting function is not too high. The controller is simple in order to solve it. So we choose the first-order weighting function as follows:

$$W_i(s) = c_i \frac{b_i s + 1}{a_i s + 1} \quad i = S, R, T \quad (24)$$

The choice of weighting function needs iterative computation. In this paper, W_S, W_R, and W_T are obtained by simulation as

$$\begin{aligned} W_S &= \begin{bmatrix} \frac{0.01}{200s+20} & & & & \\ & \frac{1}{50s+100} & & & \\ & & \frac{1}{50s+100} & & \\ & & & 1 & \\ & & & & 1 \end{bmatrix} \\ W_R &= 0.0001, \\ W_T &= \begin{bmatrix} \frac{s+50}{0.1s+5} & & & & \\ & \frac{s+10}{10s+500} & & & \\ & & \frac{1}{5s+100} & & \\ & & & 1 & \\ & & & & 1 \end{bmatrix} \end{aligned} \quad (25)$$

According to the controlled object and the generalized weighting function selected, the controller $K(s)$ is solved by using the MATLAB robust toolbox [25].

4. Simulation Results

In order to verify the control strategy to improve the EPS road sense and effect on vehicle handling performance, this paper builds a EPS simulation framework according to the control model of the system and the hybrid sensitivity H_∞ control model. It is shown in Figure 4.

In the figure, d_s and d_r are, respectively, sensor noise and road interference. $\omega_r{}^*$ is ideal yaw rate. $K_{\omega r} = u/(L(1 + Ku^2))$ is steady-state yaw angle velocity function. $K =$

Table 1: Simulation experimental parameters.

Parameter name	Variable name	Unit	Numerical value
Torsional rigidity of motor sensor	K_s	N m/rad	90
Back EMF coefficient	K_b	v s	0.02
Motor torque coefficient	K_a	N m/A	0.02
Steering wheel moment of inertia	J_h	kg m^2	0.04
Equivalent moment of inertia	J_p	kg m^2	0.06
Equivalent damping coefficient of steering shaft	B_h	N m/(rad s^{-1})	0.25
Small gear equivalent damping coefficient	B_p	N m/(rad s^{-1})	0.3
Motor armature resistance	R_a	Ω	0.01
Mass of vehicle	m	kg	1296
The moment of inertia around the plumb shaft of vehicle	I_z	kg m^2	1750
Cornering stiffness of front wheel	k_1	N/rad	95707
Cornering stiffness of rear wheel	k_2	N/rad	84243
The distance from the front wheel to the center of mass	a	m	1.25
The distance from the rear wheel to the center of mass	b	m	1.32
Coefficient of pavement interference intensity	δ_0		0.2
Front wheel trailing distance	d	m	0.1

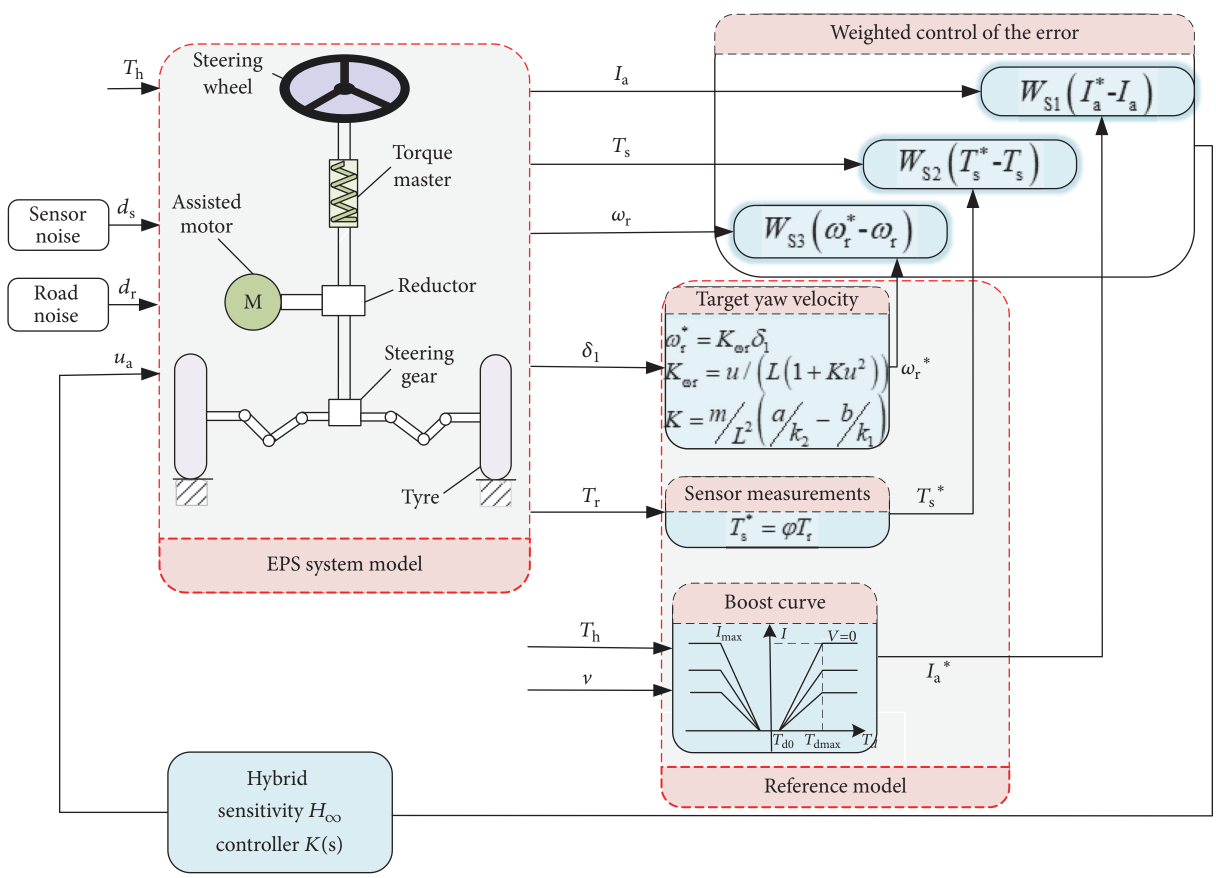

Figure 4: EPS hybrid sensitivity H_∞ control system structure diagram.

$(m/L^2)(a/k_2 - b/k_1)$ is stability factor. The ideal yaw rate can be calculated in this way: $\omega_r{}^* = K_{\omega r}\delta_1$. $T_s{}^*$ is ideal torque sensor measurement. φ is coefficient of road inductance. The ideal torque sensor has a φ times relationship with the measured resistance torque [24]. It is shown as $T_s{}^* = \varphi T_r$. $I_a{}^*$ is ideal current. The steering wheel torque is manipulated by hand, and the ideal target current is calculated by the boost characteristic curve.

The selection of simulation experiment parameters is shown in Table 1.

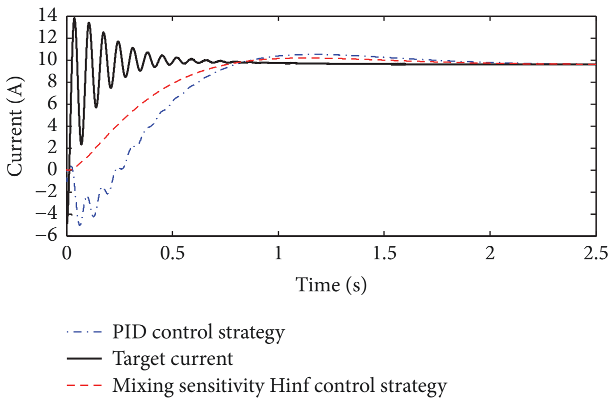

FIGURE 5: Comparison diagram of current tracking response.

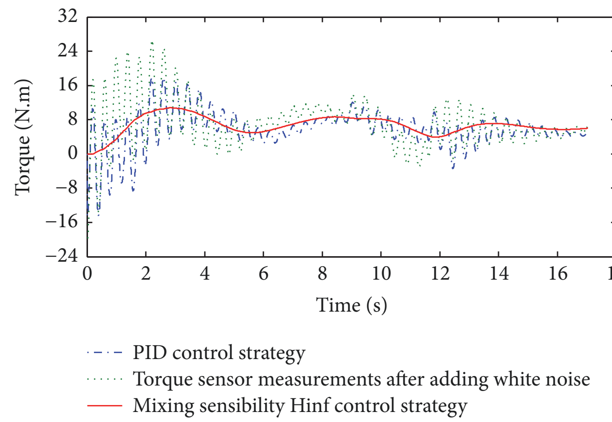

FIGURE 6: Torque sensor measurement response comparison chart.

4.1. Current Tracking Performance. The tracking speed of the actual current of the controlled motor to the target current and the tracking performance determine the response performance of EPS system. The tracking condition of the target current is observed by a step signal of the steering system. Figure 5 is the tracking response of the actual current of the controlled motor to the target current under the PID control strategy and the hybrid sensitivity H_∞ control strategy, respectively.

It can be seen from Figure 5, due to the influence of system stiffness and damping, the step signal will generate about 0.5s oscillation of the target current of the system. When the motor current of PID control is tracking the target, it will generate a certain amount of oscillation in 0-0.5 s and the response time is relatively long. There is a certain overshoot in the time of 0.8-2 s. In addition, the hybrid sensitivity control can eliminate jitter; meanwhile, it can respond more quickly and it has a good effect on tracking current.

4.2. Road Feeling. Road sense is the steering wheel torque that the driver feels during the manipulation of the vehicle. It is represented by the measurement value of the torque sensor to a certain extent. This paper mainly tests the effect of the controller on filtering interference by inputting the step response of the road and adding the noise of the road and the sensor. Set the road step as $\delta(t) = 7\ \mathrm{N} \cdot m$ to simulate. Simulation results of step response under PID control and hybrid sensitivity H_∞ control are obtained. They are shown in Figure 6.

It can be seen from Figure 6 that the measurement value of the torque sensor of PID control can track the target current very well, but it cannot eliminate the influence of jamming noise which makes the driver's road feeling worse. Compared with PID control, torque sensor measurement value controlled by hybrid sensitivity H_∞ control can effectively eliminate the influence of jamming noise, lower overshoot, and shorten the stability time, so that the driver can have a better sense of road in all kinds of interferences and noises.

4.3. Handling Stability. Yaw velocity of the vehicle is the main performance index of the vehicle steering stability.

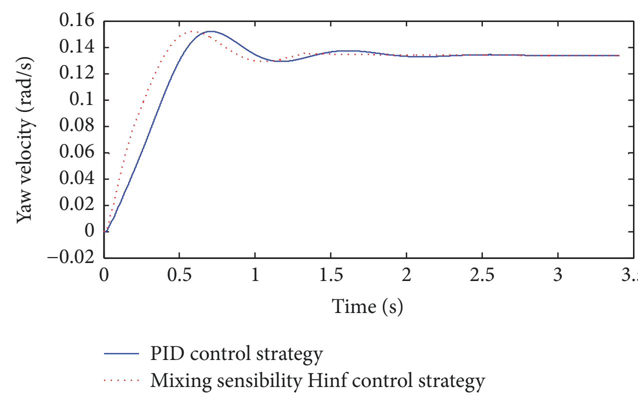

FIGURE 7: Comparison of step response of yaw rate.

The stability of the vehicle under the control strategy can be verified by the change of the angular velocity of the pavement when road step is added. As shown in Figure 7, when the speed is set to 30 m/s, the yaw velocity under the hybrid sensitivity control and the PID control is changed as shown.

Figure 7 shows that the yaw velocity of the PID control is about 7% overshoot in the 0.5-1 s period and a longer stability time is needed, which makes the vehicle's handling stability worse. The design of hybrid sensitivity H_∞ control of yaw velocity response can be very stable and response very quickly. This ensure the vehicle yaw velocity response to the driver's control command be fast and accurate. At the same time, it can improve the handling and stability of vehicle.

5. A Hybrid Sensitivity Robust Controller Is Added to the EPS System Experiment

In the simulation test section, hybrid sensitivity H_∞ controller is verified to a certain extent. In this section, the designed hybrid sensitivity H_∞ controller is embedded into the built EPS test bench [26, 27], and the designed controller mainly investigates the tracking situation of the actual

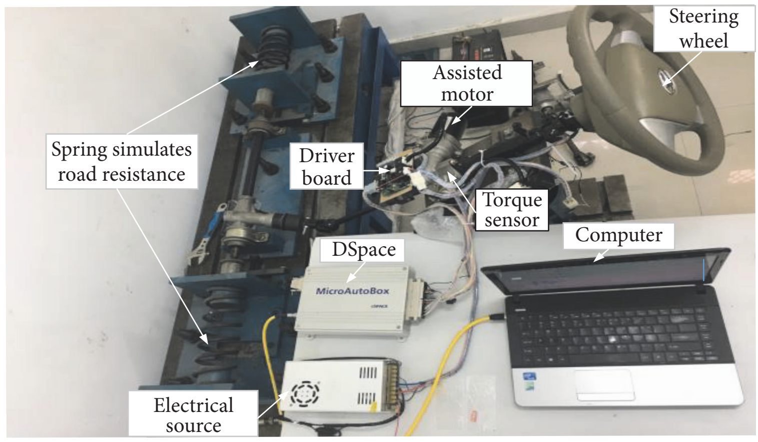

Figure 8: EPS system test bench.

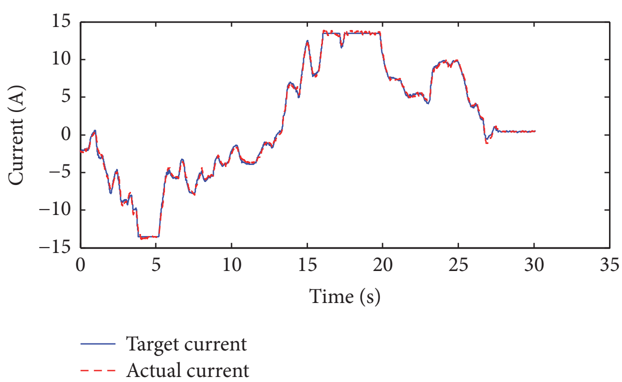

Figure 9: Hybrid sensitivity H_∞ control current tracking curve when in turn.

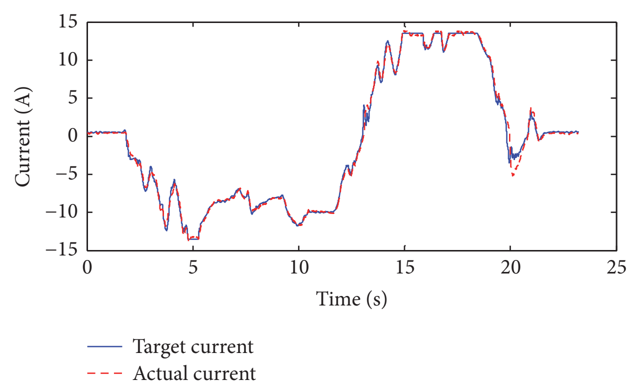

Figure 10: PID control current tracking curve when in turn.

current to the target current to verify the performance of the controller [28]. EPS test bench is shown in Figure 8. In situ simulation conditions, the torque is applied to the steering wheel. The tracking data of the actual current to the target current is recorded in real time by DSpace software control desk [29]. The power performance of EPS system under hybrid sensitivity H_∞ controller and PID controller is analyzed and compared. The test results are shown in Figures 9 and 10.

When turning in the same place, it can be seen from Figure 9 that the curve tracking of actual current to target current is almost coincident with the hybrid sensitivity H_∞ controller. It has achieved good tracking performance. As can be seen from Figure 10, the tracking curve of actual current to target current fluctuates under PID control, especially in 13 and 20 seconds, and is not ideal. The experimental results show that the proposed hybrid sensitivity H_∞ control strategy is better than the PID power assisted control strategy. It can ensure both robustness and good performance. Compared with the EPS system under the PID control, the EPS system under the hybrid sensitivity H_∞ control can have faster response speed, better robustness, and better performance.

6. Conclusion

(A) This paper establishes the mathematics model of EPS system and it takes better tracking performance of current, better driver's sense of road, and better handling stability as the control targets. The state space equation of the system is constructed by using modern cybernetics, and a hybrid sensitivity H_∞ controller is designed.

(B) To verify the design of hybrid sensitivity H_∞ controller, the simulation model is built. The simulation results show that the designed controller has good current tracking, which can guarantee that the driver has a good sense of road and can make the vehicle have good maneuvering stability. It can effectively suppress the noise and can improve the system performance while ensuring the robustness and robustness stability of the system compared with the PID controller.

(C) To verify the control effect of the controller, it is embedded into experimental bench experiments. The experimental results show that the design controller can realize the current tracking in the actual system and improve the performance, robustness, and robustness stability of the system compared with PID control.

(D) In this paper, the main factors affecting EPS system are mainly considered. The change of the system stiffness, the perturbation of the motion, and the parameters of the system are not considered. The next step will be to take more overall consideration of more indicators to establish a more eligible control system.

Conflicts of Interest

The authors declare that there are no conflicts of interest regarding the publication of this paper.

Acknowledgments

The authors acknowledge the support from Natural Science Foundation of Shandong Province (ZR2016EEQ06).

References

[1] W. Shufeng, *Automobile Structure*, 285-304, National defense industry press, Beijing, China, 2013.

[2] T. Guangxing, J. Wenguo, G. Yuan, and L. Shan, "EPS control simulation study based on immune fuzzy PID," *Computer Simulation*, vol. 31, no. 9, pp. 170–173, 2014.

[3] Z. Jianwei, X. Shijie, and Q. Baojun, "Research and simulation of control strategy for electric power steering system," *Machine Tool & Hydraulics*, vol. 44, no. 6, pp. 96–100, 2016.

[4] Q. Ming, Y. Jiajun, L. Zhao, and Y. Geng, "Research of electric power steering system based on H_∞ robust control theory," *Journal of Huazhong University of Science and Technology (Natural Science Edition)*, vol. 30, no. 12, pp. 72-73, 2002.

[5] W. Qirui, C. Wuwei, H. Sengren, and Y. Ming, "Research on H_∞ control of automotive electric power steering system," *Automobile Engineering*, vol. 26, no. 5, pp. 609–612, 2004.

[6] Z. Wanzhong, S. Guobiao, L. Yi, and L. Qiang, "Steering sense of electric power assisted system based on hybrid H_2/H_∞ control," *Chinese Journal of Mechanical Engineering*, vol. 45, no. 4, pp. 142–147, 2009.

[7] W. Jingliang and Y. Yunbing, "Robust control strategy of EPS steering system based on handling stability," *Journal of Wuhan University of Science and Technology*, vol. 37, no. 3, pp. 204–209, 2014.

[8] S. Guoqin and Y. Yunbing, "Research on H_∞ robust control of electric power steering system and its influence on handling stability," *Modern Manufacturing Engineering*, vol. 9, pp. 114–120, 2016.

[9] C. Long, Y. Chaochun, and J. Haobin, "Study on the stability of EPS vehicle based on μ integrated robust control," *Automotive Engineering*, vol. 30, no. 8, pp. 705–712, 2008.

[10] F. Wilhelm, T. Tamura, R. Fuchs, and P. Mullhaupt, "Friction compensation control for power steering," *IEEE Transactions on Control Systems Technology*, vol. 24, no. 4, pp. 1354–1367, 2016.

[11] Y.-C. Hung, F.-J. Lin, J.-C. Hwang, J.-K. Chang, and K.-C. Ruan, "Wavelet fuzzy neural network with asymmetric membership function controller for electric power steering system via improved differential evolution," *IEEE Transactions on Power Electronics*, vol. 30, no. 4, pp. 2350–2362, 2015.

[12] W. Kim, Y. S. Son, and C. C. Chung, "Torque overlay-based robust steering wheel angle control of electrical power steering for a lane-keeping system of automated vehicles," *IEEE Transactions on Vehicular Technology*, vol. 10, no. 1109, pp. 1–14, 2015.

[13] A. Marouf, M. Djemai, C. Sentouh, and P. Pudlo, "A new control strategy of an electric-power-assisted steering system," *IEEE Transactions on Vehicular Technology*, vol. 61, no. 8, pp. 3574–3589, 2012.

[14] D. Lee, K.-S. Kim, and S. Kim, "Controller design of an electric power steering system," *IEEE Transactions on Control Systems Technology*, 2018.

[15] C. T. Faria, G. Pulvirenti, and T. Geluk, "Modeling and non-linear parameter identification of an electric-power steering system," in *Topics in Modal Analysis & Testing*, pp. 127–135, The Society for Experimental Mechanics, 2017.

[16] Y. Zhisheng, *Automobile Theory*, Mechanical Industry Press, Beijing, China, 2000.

[17] C. Yin, Q. Sun, J. Wu, C. Liu, and J. Gao, "Development of electrohydraulic steering control system for tractor automatic navigation," *Journal of Electrical and Computer Engineering*, vol. 2018, Article ID 5617253, 7 pages, 2018.

[18] A. Baier, K. Herbuś, P. Ociepka, and M. Płaczek, "Modal analysis in relation to the casing of an electric power steering system," in *Proceedings of the IOP Conference Series: Materials Science and Engineering*, vol. 227, pp. 1–8, June 2017.

[19] Y. Li, T. Shim, D. Wang, and T. Offerle, "Comparative Study of Rack Force Estimation for Electric Power Assist Steering System," in *Proceedings of the ASME 2017 Dynamic Systems and Control Conference*, vol. 5255, pp. 1–8, Tysons, Virginia, USA, 2017.

[20] W. Z. Zhao, Y. J. Li, C. Y. Wang, Z. Q. Zhang, and C. L. Xu, "Research on control strategy for differential steering system based on H_∞ hybrid sensitivity," *International Journal of Automotive Technology*, vol. 14, no. 6, pp. 913–919, 2013.

[21] S. Tielong, *H_∞ Control theory and application 2*, Tsinghua University press, Beijing, China, 2008.

[22] Oppenheim, *Signals and Systems*, Electronic Industry Press, Beijing, China, 2013.

[23] M. Shengwei, S. Tielong, and L. Kangzhi, *Modern robust control theory and its application*, Tsinghua University press, Beijing, China, 2003.

[24] Z. Huaiquan and G. Jia, "Research on EPS handling stability based on H_∞ hybrid sensitivity control," *Journal of Beijing Institute of Technology*, vol. 32, no. 12, pp. 1252–1257, 2012.

[25] J. G. Michael, *Model predictive control system design and implementation using matlab*, Industrial Control Centre, Glasgow, Scotland, UK, 2015.

[26] H. Zheng and M. Zhao, "Development a HIL test bench for electrically controlled steering system," *SAE Technical Papers*, vol. 01, no. 51, pp. 1–7, 2016.

[27] X. Li and Y. Li, "Research and development of the simulation platform of the nose wheel with digital steering system based on hardware in the loop," in *Proceedings of the 2016 IEEE/CSAA International Conference on Aircraft Utility Systems, AUS 2016*, pp. 729–733, Beijing, China, October 2016.

[28] Z. Zhiguo, Y. Zhuoping, S. Zechang, and C. Hui, "Research on H_∞ robust control of electric power steering system," *Automobile Engineering*, vol. 27, no. 6, pp. 730–735, 2005.

[29] Z. Zhiming, *Automotive electric power steering system control algorithm and dSPACE real-time simulation study*, W. Han, Ed., Huazhong University of Science and Technology, 2007.